Journal of Maps

ISSN: 1744-5647 (Online) Journal homepage: www.tandfonline.com/journals/tjom20

Salt diapirism constrained by the stratigraphical record of adjacent basins: the Estopanyà Syncline (South-Central Pyrenees, NE Iberian Peninsula)

Pedro Ramirez-Perez, Gabriel Cofrade, Mercè Estiarte-Ruiz, Juan Diego Martín-Martín, Antonio Teixell & Anna Travé

To cite this article: Pedro Ramirez-Perez, Gabriel Cofrade, Mercè Estiarte-Ruiz, Juan Diego Martín-Martín, Antonio Teixell & Anna Travé (2025) Salt diapirism constrained by the stratigraphical record of adjacent basins: the Estopanyà Syncline (South-Central Pyrenees, NE Iberian Peninsula), Journal of Maps, 21:1, 2525925, DOI: 10.1080/17445647.2025.2525925

To link to this article: https://doi.org/10.1080/17445647.2025.2525925

JOURNAL OF MAPS
2025, VOL. 21, NO. 1, 2525925
https://doi.org/10.1080/17445647.2025.2525925

Taylor & Francis
Taylor & Francis Group

Science

OPEN ACCESS Check for updates

Salt diapirism constrained by the stratigraphical record of adjacent basins: the Estopanyà Syncline (South-Central Pyrenees, NE Iberian Peninsula)

Pedro Ramirez-Perez [a], Gabriel Cofrade [a], Mercè Estiarte-Ruiz [b], Juan Diego Martín-Martín[a], Antonio Teixell [c] and Anna Travé [a]

[a]Institut de Recerca Geomodels-UB, SGR Geologia Sedimentària, Departament de Mineralogia, Petrologia i Geologia Aplicada, Facultat de Ciències de la Terra, Universitat de Barcelona (UB), Barcelona, Spain; [b]Institut de Recerca Geomodels-UB, Grup de Geodinàmica i Anàlisi de Conques (GGCA), Departament de Dinàmica de la Terra i de l'Oceà, Facultat de Ciències de la Terra, Universitat de Barcelona (UB), Barcelona, Spain; [c]Departament de Geologia, Universitat Autònoma de Barcelona (UAB), Bellaterra, Spain

ABSTRACT

The detailed geological mapping of structural and stratigraphical patterns within the sedimentary succession of the Estopanyà Syncline (South-Central Pyrenees) and surrounding structures provides insights into the evolution of the adjoining diapirs. The present-day stratigraphical and geometric relationships between the diapirs and flanking sedimentary units suggest distinct halokinetic evolution in the ESE and WNW sectors of the studied area. In the ESE sector, flanking successions are characterized by halokinetic breccias and overturned layer attitudes, indicative of an early salt inflation phase during the Late Cretaceous. The advance of the pyrenean compressional front produced the extrusion of these diapirs during the middle Ypresian. In the WNW sector, salt diapirism occurred lately, during the middle Eocene to Oligocene, due to the rotation of the Estopanyà Syncline and the welding of the pre-existing diapirs.

ARTICLE HISTORY
Received 21 January 2025
Revised 18 June 2025
Accepted 19 June 2025

KEYWORDS
Salt basin; diapirism; salt wall; stratigraphy; Pyrenees

1. Introduction

Rheological properties of salt are especial compared to other sedimentary rocks as, under certain temperature and pressure conditions, salt deforms ductile allowing it to flow (i.e. diapirism, Urai et al., 2008). During diapirism salt migrate to low pressure areas where it can be accumulated or expulsed forming a variety of related structures, generally known as diapirs (e.g. Jackson & Hudec, 2017; Jackson & Talbot, 1986). When possible, diapirs can be distinguished according to their shape, been cylindrical or elongated shapes the most common (i.e. salt plugs or salt walls, respectively). Salt flow results in the reshaping of the adjacent topography, altering the geometry and position of surrounding sedimentary basins (Andrie et al., 2012; Counts et al., 2019; Kalifi et al., 2023; Ribes et al., 2016). Thereby, salt diapirism leaves a distinctive imprint on the contemporaneous stratigraphical record through the deposition of characteristic sedimentary facies and stratal patterns such as diapir margin breccias and halokinetic sequences (Pichel & Jackson, 2019; Rowan et al., 2022). Interpretation of these facies can be used to reconstruct the evolution of currently deformed complex diapirs. For instance, in orogenic belts like the Pyrenees tectonic shortening can obscure the original geometry of pre-existing diapirs by squeezing them, which results in secondary welding, extrusion, and subsequent salt dissolution. These processes commonly affect diapirs during mountain building, which difficult to reconstruct their position, shape, and dimensions before orogenic compression and to consider their role in the orogenic evolution (Duffy et al., 2018; Muñoz et al., 2024; Santolaria et al., 2021, 2022). Moreover, deformation produces complex diapir geometries that difficult to model, without well-established field analogues, these structures for their use as, for example, for energy purposes such as the emplacement of hydrogen salt caverns or geothermal reservoirs (e.g. Duffy et al., 2023; Ramirez-Perez et al., 2025).

One proved strategy to reconstruct diapirs involves mapping the present-day geometry of salt exposures and identify distinctive stratigraphical and sedimentological patterns in the adjacent basins, as made in the Moroccan Atlas (Martín-Martín et al., 2017; Moragas et al., 2019; Saura et al., 2014; Teixell et al., 2017; Vergés et al., 2017), the Australian Flinders Range (Rowan, 2017; Vidal-Royo et al., 2021), or the Pyrenees itself (Burrel & Teixell, 2021; Cofrade, Cantarero, et al., 2023; Cofrade, Gratacós, et al., 2023; Kalifi et al., 2023; Poprawski et al., 2016; Ramirez-Perez et al.,

CONTACT Pedro Ramirez-Perez pramirezperez@ub.edu Institut de Recerca Geomodels-UB, SGR Geologia Sedimentària, Departament de Mineralogia, Petrologia i Geologia Aplicada, Facultat de Ciències de la Terra, Universitat de Barcelona (UB), Barcelona, Spain
Supplemental map for this article can be accessed online at https://doi.org/10.1080/17445647.2025.2525925.

2024; Roca et al., 2016; Saura et al., 2016). To adequately constrain the geometry and nature of diapirs, geological maps should be adjusted to match the scale of expected halokinetic-driven disruptions such as localized rapid facies changes and complex folds and faults patterns (Pichel & Jackson, 2019; Poprawski et al., 2016).

The study of diapirism of the Triassic unit (Middle and Upper Triassic Muschelkalk and Keuper facies) in the Southern Pyrenees traditionally focused on the northern part of the fold-and-thrust belt, defining post-rift (Lower Cretaceous) diapirs that were deformed during the Pyrenean orogeny (Late Cretaceous–Miocene) (e.g. Burrel et al., 2021; Casini et al., 2023; Gannaway Dalton et al., 2022; García-Senz et al., 2024; López-Mir et al., 2014, 2015; Saura et al., 2016). However, the southernmost part of the Southern Pyrenees also hosts several diapirs which remained less studied until recent years (e.g. Burrel & Teixell, 2021; Cofrade, Cantarero, et al., 2023; Cofrade, Závada, et al., 2023; Ramirez-Perez et al., 2024; Santolaria et al., 2014, 2016, 2020, 2022). In this contribution, we constrain the evolution of the Estopanyà Syncline in the frontal part of the Serres Marginals Thrust Sheet in the South-Central Pyrenees presenting a new 1:28,500 geological map of the area. Detailed mapping, combined with new structural, stratigraphical, sedimentological, and petrological data, enables to interpret the evolution of adjacent diapirs during the Pyrenean orogeny, providing a field study to be used as an analogue for similar salt basins worldwide.

2. Geological setting

The Pyrenees are a doubly verging Alpine orogen formed during the Late Cretaceous to Miocene collision between the Iberian and Eurasian plates, which inverted the previously existing Lower Cretaceous hyperextended margin (Beaumont et al., 2000; Labaume & Teixell, 2020; Mouthereau et al., 2014; Muñoz, 1992; Pedrera et al., 2023; Teixell et al., 2018). This orogen is characterized by a central zone formed by an antiformal stack of basement-involved thrusts (Axial Pyrenean Zone) flanked by two opposite verging fold-and-thrust belts (North and South Pyrenean Zones) that were emplaced over their respective autochthonous foreland basins (Aquitaine and Ebro Basins, Figure 1).

In the South Pyrenean Zone (SPZ), compressional deformation migrated southwards forming a thrust sequence detached over the Upper Triassic evaporites and mudrocks of the Keuper facies. The thrust sequence is represented by the Bóixols Thrust Sheet (emplaced during Santonian–Campanian), Montsec Thrust Sheet (during Maastrichtian–Paleocene), and Serres Marginals Thrust Sheet (during Middle Eocene–Oligocene) (Casini et al., 2023; Cruset et al., 2023; Ford et al., 2022; Meigs, 1997; Puigdefàbregas et al., 1986, 1992; Séguret, 1972; Teixell & Muñoz, 2000; Vergés & Munoz, 1990) (Figure 2). The displacement of the orogenic belt is larger in the central part of the SPZ than in other parts due to the uneven distribution of the Keuper facies and the occurrence of a secondary detachment level in the foreland (the Eocene–Oligocene evaporites of the Barbastro Fm, Santolaria et al., 2015; Teixell & Muñoz, 2000; Vergés et al., 1992) (Figure 1). This formed an orogenic salient known as the South-Central Pyrenean Thrust Salient (SCPTS, Angrand et al., 2020; Muñoz et al., 2013, 2024; Santolaria, Ayala, et al., 2024; Santolaria, Izquierdo-Llavall, et al., 2024). The studied Estopanyà Syncline is located in the western margin of the SCPTS, in the frontal part of the Serres Marginals Thrust Sheet (SMTS, Figure 1).

The diapirs in the SMTS (e.g. Jusseu, Puebla de Castro, Les Avellanes diapirs) are sourced from mudrocks, carbonates, and gypsum of the Upper Triassic Keuper facies (K1 and K2), which constitute an original Layered Evaporite Sequence (Triassic LES) that also act as the main detachment level in the Pyrenees (Burrel & Teixell, 2021; Casas et al., 2016; Cofrade, Cantarero, et al., 2023; Santolaria et al., 2014). During diapirism, the intrasalt carbonates (referred here as Muschelkalk carbonates) and dolerite bodies were disrupted and incorporated into the diapirs as stringers (Cofrade, Cantarero, et al., 2023; Cofrade, Závada, et al., 2023). The current diapir exposures are formed by an amalgamation of intensely deformed caprock matrix (mudrocks and gypsum) and less deformed competent stringers (carbonates, breccias, and dolerites, Figure 2). The most soluble salts (halite and other chlorides) have been dissolved near the surface, but they are reported in depth from borehole and gravimetric data (Lanaja, 1987; Santolaria, Ayala, et al., 2024).

The non-diapiric sedimentary cover in the SMTS is divided into a pre-orogenic and a syn-orogenic sequence with a complete absence of the Lower Cretaceous stratigraphy (Pocoví, 1978) (Figure 2). The pre-orogenic sequence (Triassic–Jurassic) pinches out progressively towards the south and west of the SMTS, with its maximum thickness in the Montroig-Camarasa sector (1000 m, Jurado, 1990; Ortí et al., 2017; Salvany, 2017). In the Estopanyà Syncline, the thickness of the pre-orogenic sequence is greatly reduced (60–150 m) and includes the mudrocks of the K3 facies (Late Triassic), the oolitic dolostones of the Isàbena Fm (Rhaetian), and the intraformational breccias of the Cortes de Tajuña Fm (Hettangian) (Ramirez-Perez et al., 2024).

The syn-orogenic sequence (late Santonian–Oligocene) postdates a significant sedimentary hiatus (the Santonian Unconformity). This unconformity is

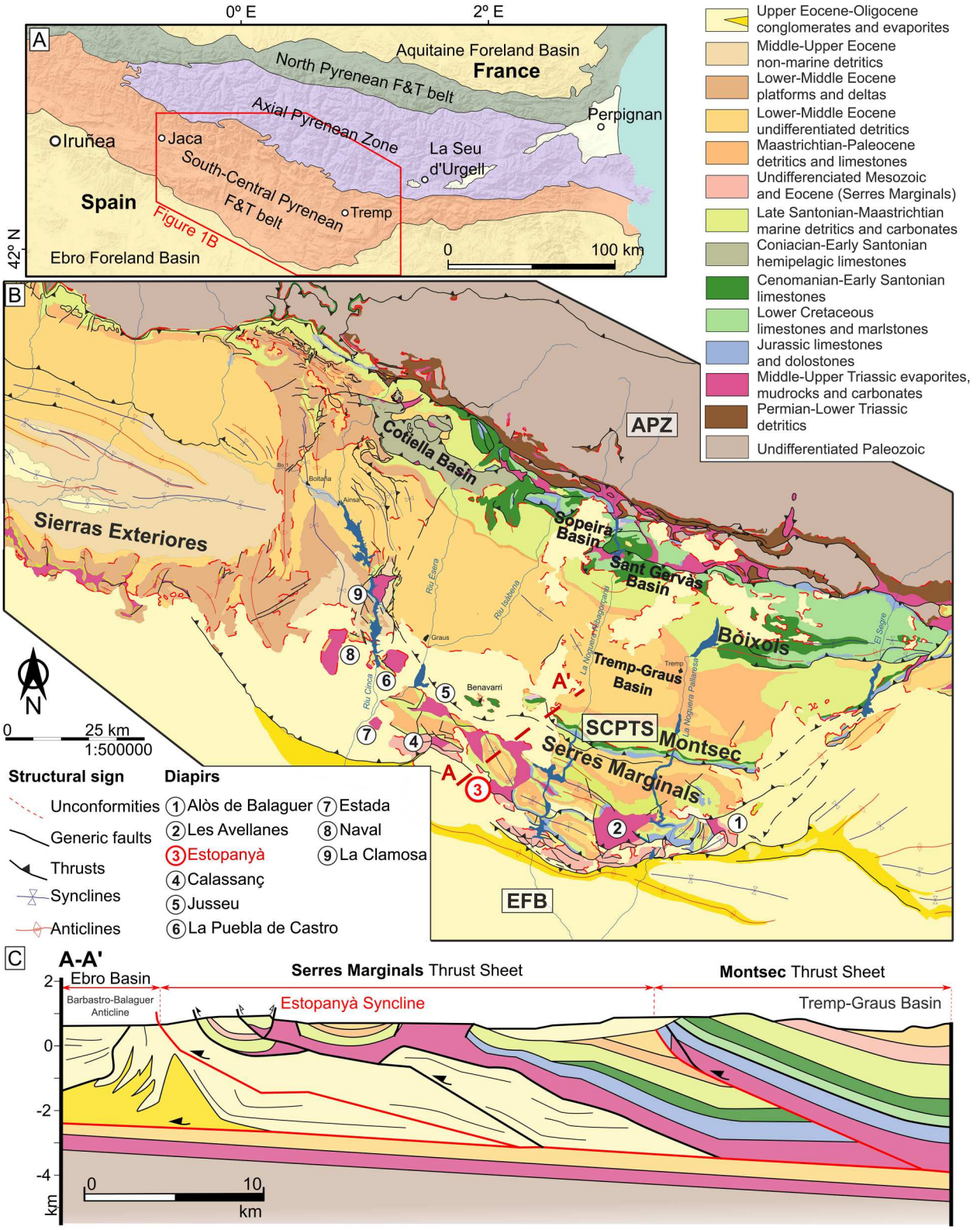

Figure 1. Tectonic and geological framework of the South-Central Pyrenees. (A) Synthetic geological map of the Pyrenees showing the central Axial Pyrenean Zone (APZ), the two opposite-verging Fold-and-Thrust Belts, and their respective foreland basins (modified from González-Esvertit et al., 2022). (B) Geological map of the South-Central Pyrenean Thrust Salient (SCPTS), which includes the piggy-back thrust sequence of the Bòixols, Montsec, and Serres Marginals Thrust Sheets, emplaced over the autochthonous Ebro Foreland Basin (EFB). Numbers indicate the location of diapirs within the Serres Marginals Thrust Sheet (modified from Muñoz et al., 2018). (C) Cross-section from the Montsec Thrust Sheet to the Ebro Foreland Basin based on gravimetric and structural data (modified from Santolaria, Ayala, et al., 2024; after Senz & Zamorano, 1992).

associated with the tectonic inversion, uplift, and erosion at the beginning of the Pyrenean orogeny (Garrido-Megias, 1973; Pocoví, 1978) (Figure 2). The first unit overlying this hiatus in the Estopanyà Syncline is the Adraén Fm (late Santonian), followed by the marine Terradets Fm (Campanian–

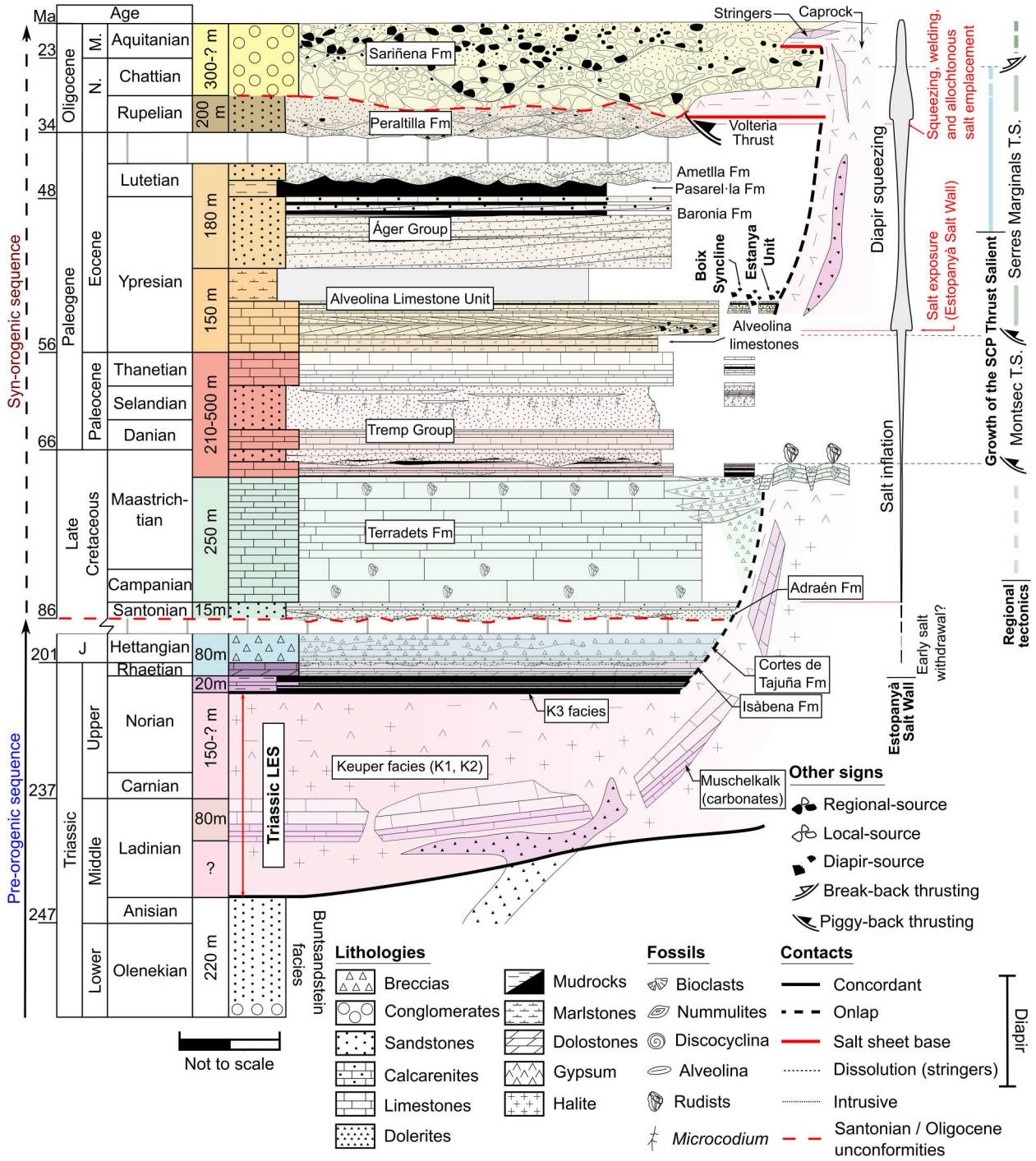

Figure 2. Lithostratigraphical chart units and relationship with diapirism in the studied area, (after Ramirez-Perez et al., 2024). The thickness of the Triassic LES is uncertain in the Serres Marginals Thrust Sheet due to thrusting and diapirism. The Oligocene succession is modified from that reported by Garrido-Megías (1972) and Senz and Zamorano (1992). The left side of the figure summarizes the main tectonic events of the South Pyrenean Zone, including diapirism in the Estopanyà Syncline, with correlation lines associating these events with their coetaneous sedimentary units.

Maastrichtian). The Late Cretaceous–Paleocene transition is recorded by the terrestrial Garumnian facies, exhibiting a general regressive trend compared to the preceding Late Cretaceous sequence. During the late Thanetian, a major marine transgression occurred in the SMTS. The stratigraphical signature of this transgression is the deposition of the Alveolina Limestone Unit (Ypresian), which in Estopanyà comprises three members as described by Ramirez-Perez et al. (2024) (Figure 2). The remaining Eocene succession includes the deltaic Àger Group, which consists of the Baronia (middle Ypresian), Pasarel·la (upper Ypresian), and Ametlla (upper Ypresian–Lutetian) Fms (Figure 2). Eocene units in Estopanyà are postdated by the Peraltilla Fm (Lower Oligocene) that was deposited during the emplacement of several internal thrusts in the Serres Marginals Thrust Sheet (e.g. Volteria Thrust, Garrido-Megias, 1973; Meigs, 1997; Teixell & Barnolas, 1996). The top of the Peraltilla Fm marks another regional unconformity in the

SMTS, referred to as the Oligocene Unconformity (Figure 2). This unconformity is overlain by the Upper Oligocene–Lower Miocene conglomerates and sandstones of the Sariñena Fm, which extends throughout the SPZ and into the Ebro Basin recording the latest out-of-sequence thrusts (Teixell & Barnolas, 1996) (Figures 1 and 2).

Based on the stratigraphical and sedimentological study of the basin-filling sedimentary units in the eastern limb of the Estopanyà Syncline, Ramirez-Perez et al. (2024) proposed a Late Cretaceous to Oligocene diapir evolution for the Estopanyà and Boix Synclines (Figure 2). Accordingly, present-day salt exposures in Estopanyà evolved from buried salt walls that disrupted the Late Cretaceous carbonate platforms growing atop. This process led to the erosion of these platforms resedimenting them as breccias in the adjacent basins. The progressive growth of salt structures diminished the sedimentation of the Paleocene succession in the Boix Syncline, resulting in a more condensed stratigraphical record (Main Map, Figure 2). During the Ypresian, the deposition of diapir-derived euhedral quartz grains containing anhydrite inclusions within the Alveolina Limestone Unit indicates the presence of exposed diapirs near the Estopanyà and Boix Synclines. Probably, the internally accommodated shortening in the SMTS associated to its emplacement (Middle Eocene–Oligocene), triggered the squeezing of pre-existing diapirs leading to high extrusion rates that was further enhanced by the Oligocene break-back reactivation. This shortening caused a main diapiric phase in the frontal part of the SMTS, promoting salt expulsion and welding (Burbank et al., 1992; Burrel & Teixell, 2021; Teixell & Muñoz, 2000).

3. Methods

The geological map presented in this study, the Main Map, covers an area of 196 km^2 and it is presented at 1:28,500 scale. The cartographic work was developed at 1:10,000 scale combining Remote Sensing Mapping techniques based on the interpretation of high-resolution LiDAR data, DEM, and available orthophotographs and extensive fieldwork along the exposed margins of the Estopanyà Salt Wall and the Estopanyà Syncline, which are better preserved in the eastern part of the Main Map (see Supplementary Material). The Main Map is based on previously published geological maps from the IGME's Mapa Geológico Nacional 1:50,000 series, including the Fonz sheet (Teixell et al., 1994), Monzón sheet (García-Senz et al., 1990), Benabarre sheet (Vilar, 1996), Os de Balaguer sheet (Teixell & Barnolas, 1996), as well as additional regional maps (Burrel & Teixell, 2021; Cofrade, Gratacós, et al., 2023; Muñoz et al., 2018). Data from previous maps was simplified to represent the best the focus of this study, the geological reinterpretation of the Estopanyà Syncline. Therein, some of the previously mapped units are shown together in the Main Map and only structural and bedding data acquired during fieldwork has been included, although data from the previous maps was also considered during reinterpretation. Structural and bedding measurements were obtained directly in the field using a compass-clinometer georeferenced with FieldMove software. These data were later digitalized using QGIS (v3.26 and v3.32). The topographic base for mapping relied on two HD-DEM datasets provided by the Spanish National Geographic Institute (IGN) with resolutions of 2×2 m and 5×5 m (MDT02 and MDT05), v2.0 (2015–2021). These DEMs were combined and used as source layers for the northern and southern parts of the map, respectively. The Main Map is accompanied by a larger-scale geological map that highlights the structural context within the western termination of the South-Central Pyrenean Thrust Salient and a lithostratigraphical chart indicating the main tectonic and diapiric events observed at Estopanyà. A structural cross-section was developed following N060E azimuth in the western sector and N074E in the eastern segment to show the structural characteristics of the mapped area (cross-section I–I′, see Supplementary Material 2). In this cross-section the trace of the basal Serres Marginals Thrust has been inferred based on the previously published sections (e.g. Santolaria, Izquierdo-Lavall et al., 2024). Quaternary deposits were excluded from the final map and section.

4. Results

This contribution focuses on the Estopanyà Syncline, a NNW–SSE oriented fold flanked by extensive diapir exposures formed by Triassic salts. The major structures delimiting the study area are the Blancafort Syncline (E), the Canelles Anticline (ESE), the Tragó Syncline (S–SE), the Baldellou syncline (S), the Sant Quilez Syncline (W), and various small-scale structures to the N–NW (Figure 3).

The Estopanyà Syncline consists of a 7 km long by 2 km wide asymmetric fold showing a comparatively more steeply dipping eastern than western limb (see cross-section, Supplementary Material 2). The closures of the fold are also distinct. The northern closure is structurally more complex and characterized by several low-amplitude roughly N–S-oriented folds delimited by parallel faults and thrusts, while the southern closure shows an uninterrupted sedimentary succession. The orientation of the syncline is parallel to the main axes of the flanking structures and the trace of the Serres Marginals Thrust, that is hindered by Oligocene units in the study area. The Estopanyà Syncline is delimited at its eastern limb by the Estopanyà Salt

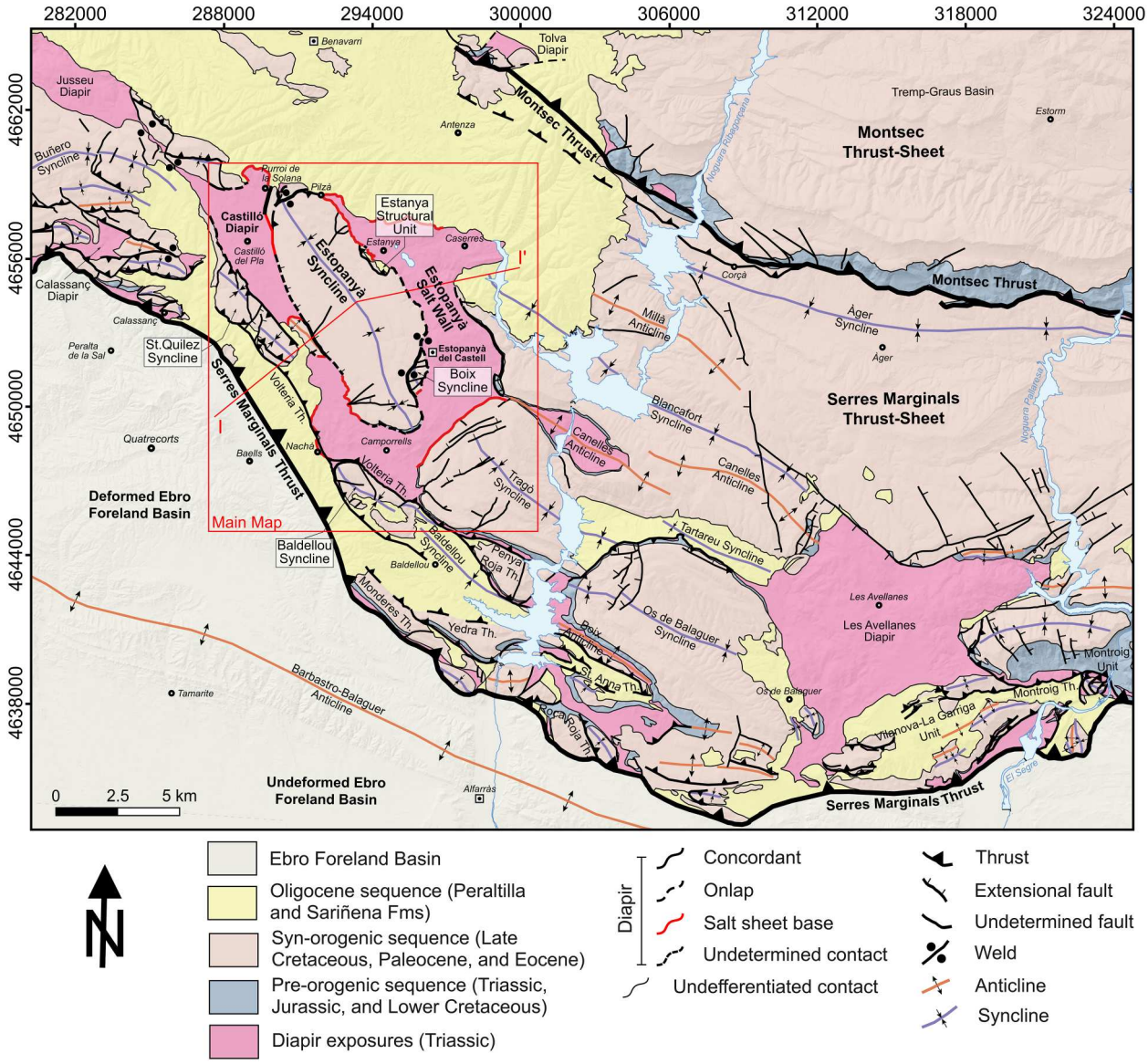

Figure 3. (A) Structural map of the western South Pyrenean Thrust Salient, highlighting key diapir exposures and structures next to the Estopanyà Syncline (ES) (modified from Cofrade, Gratacós, et al., 2023). The figure contains the trace of the Main Map area (red square), the I–I′ cross-section (Supplementary Material 2), and the most significant structures discussed in the text.

Wall and two minor-scale structures known as the Boix Syncline and the Estanya Structural Unit (Figure 3). The Estopanyà Salt Wall extends southward delimiting also the southern closure of the Estopanyà Syncline. The western limb of this syncline is characterized by a sharp contact with an upright turn anticline and the Castilló Diapir.

Attending to the stratigraphy, three principal units can be distinguished in the studied area: (1) the Triassic salts associated with diapirs that bound the Estopanyà Syncline; (2) the pre- and syn-orogenic sedimentary cover within the studied structures; and (3) the Oligocene units that onlap the study area postdating the studied diapirs and folds (Figure 3). The next section describes the structure and stratigraphy of the Estopanyà Syncline in the main parts of this fold (i.e. northern and southern closures and eastern and western limbs, Main Map), paying special attention to the observed geometries, stratigraphical contacts, and sedimentary facies.

4.1. Structure of the northern closure of the Estopanyà Syncline

The northern closure of the Estopanyà Syncline comprises the area between the Pilzà and Purroi de la Solana villages (northern sector of the Main Map, Figure 3). The closure of the syncline is characterized by an E–W oriented thrust that places the Estopanyà Syncline, in the southern hanging wall, on top of a footwall depicting Late Cretaceous and Lower to Middle Paleocene units. These units form a south-dipping panel in the westernmost part of the northern closure, but they become overturned to the east, suggesting a very verticalized fold between them. This E–W thrust passes laterally into a confined diapir

near the Pilzà village. The Triassic exposed in the northern sector is mainly formed by altered mudrocks and gypsums with scarce stringers that appear only in a small area NNW of Purroi de la Solana, depicting heterometric bodies of dolerite and Muschelkalk carbonates that override the Oligocene conglomerates in the north, forming an irregular contact between the Triassic and the Sariñena Fm at this point (Main Map).

4.2. Structure of the eastern limb of the Estopanyà Syncline

The eastern limb of the Estopanyà Syncline is limited by the NNW–SSE oriented Estopanyà Salt Wall, which forms the largest salt exposure in the study area (Figure 3). The salt wall is the NNW continuation of the Canelles Anticline and is confined to the east by the Blancafort Syncline and to the west by the Boix and Estopanyà Synclines. The northern boundary is set by the conglomerates of the Sariñena Fm, that postdate the salt wall in this point (Figure 3).

The NNW margin of the eastern limb of the Estopanyà Syncline corresponds to the Estanya Structural Unit (ESU), characterized by an east-dipping middle Ypresian succession that is emplaced by a thrust over the west-dipping Paleocene strata of the Estopanyà Syncline (Main Map). The eastern boundary of the ESU is defined by an irregular contact between folded middle Ypresian limestones and the Keuper facies of the Estopanyà Salt Wall. Stringers in this sector run parallel to the salt wall margins and exhibit a bimodal pattern: steeply dipping stringers dominate south of the Estanya village while sub-horizontal stringers prevail to the north. The latter display high-amplitude folds with a predominant WNW–ESE axes and host the unique karstic lakes in the area (the Estanya lakes).

South of the Estanya village, the trace of the Estopanyà Salt Wall is NNW–SSE, parallel to the axes of the surrounding structures (i.e. the Blancafort Syncline in the east and the Estopanyà and Boix Synclines in the west, Figure 3). In both cases, the contact between the Estopanyà Salt Wall and the flanking sedimentary units is sharp and involves halokinetic structures such as flaps, as suggested by the steeply dipping to overturned Late Cretaceous strata (Figure 4(A)). This contact in the Estopanyà and Boix Synclines also includes halokinetic sequences depicted by the deposition of monomictic breccias that wedge and steepen laterally towards the diapir, transitioning rapidly basinwards into the well-stratified, gently dipping limestones of the Terradets Fm (Ramirez-Perez et al., 2024). In the Boix Syncline, it is common to found euhedral quartz grains within the Ypresian limestones, coming from the erosion of the Keuper facies. However, these grains were not found in the Late Cretaceous breccias (Ramirez-Perez et al., 2024). Stringers in this sector of the map are comparatively more continuous than in the north, forming sub-vertical bodies with tight, often faulted, recline folds at the centre of the salt wall.

4.3. The diapir exposures of the southern closure of the Estopanyà Syncline

The southern closure of the Estopanyà Syncline comprises the area between the Camporrells and Nachá villages. It is delimited to the south by a diapir exposure that extends until the Tragó and Baldellou Synclines (southern sector of the Main Map, Figure 3). Salt exposure is predominantly NE–SW oriented, almost perpendicular to those in the eastern sector. The southern boundary of the diapir is irregular, with a salt overhang that slightly truncates the Late Cretaceous–Paleocene succession of the Tragó Syncline (Figure 3). In contrast, in the northern boundary of the diapir, the closure of the Estopanyà Syncline shows a basal pre-orogenic sequence that is concordant with the underlaying Keuper facies (Figure 4(B)). Along this contact, the Late Triassic and Jurassic units wedge laterally, placing the Late Cretaceous succession of the Estopanyà Syncline unconformably over the diapir (Figure 3). The stringers in this sector are parallel to the diapir boundary and are seen as vertical and continuous bodies.

To the west of Camporrells, the contact between the diapir exposure and the Baldellou Syncline follows the trace of the Volteria Thrust, that places the Tragó Syncline in the hanging wall on top of the Baldellou Syncline, fossilized by the Sariñena Fm in the footwall (Figure 3). The Volteria Thrust can be traced until the Sant Quilez Syncline, although it is partially obscured by the Oligocene conglomerates of the Sariñena Fm and the Triassic salt exposures of the Nachá village (Figure 4(C)). In Nachá, this salt occupies a comparatively more elevated topographic position than the surrounding Oligocene Peraltilla Fm (Figure 4(C)). However, the contact between these units is rapidly postdated to the north by the Sariñena Fm. The stringer array in Nachá consists of discontinuous bodies showing vertical to sub-horizontal dips, parallel to the salt contact. Some of the stringers were transported within the salt and are currently located over the Oligocene Peraltilla Fm (Main Map).

4.4. The diapir exposures of the western limb of the Estopanyà Syncline

The western limb of the Estopanyà Syncline encompasses the area between the Nachá and Purroi de la Solana villages. It is delimited to the west by an almost continuous salt exposure that is oriented parallelly to the axes of the Sant Quilez and Estopanyà Synclines (western sector of the Main Map). This sector is

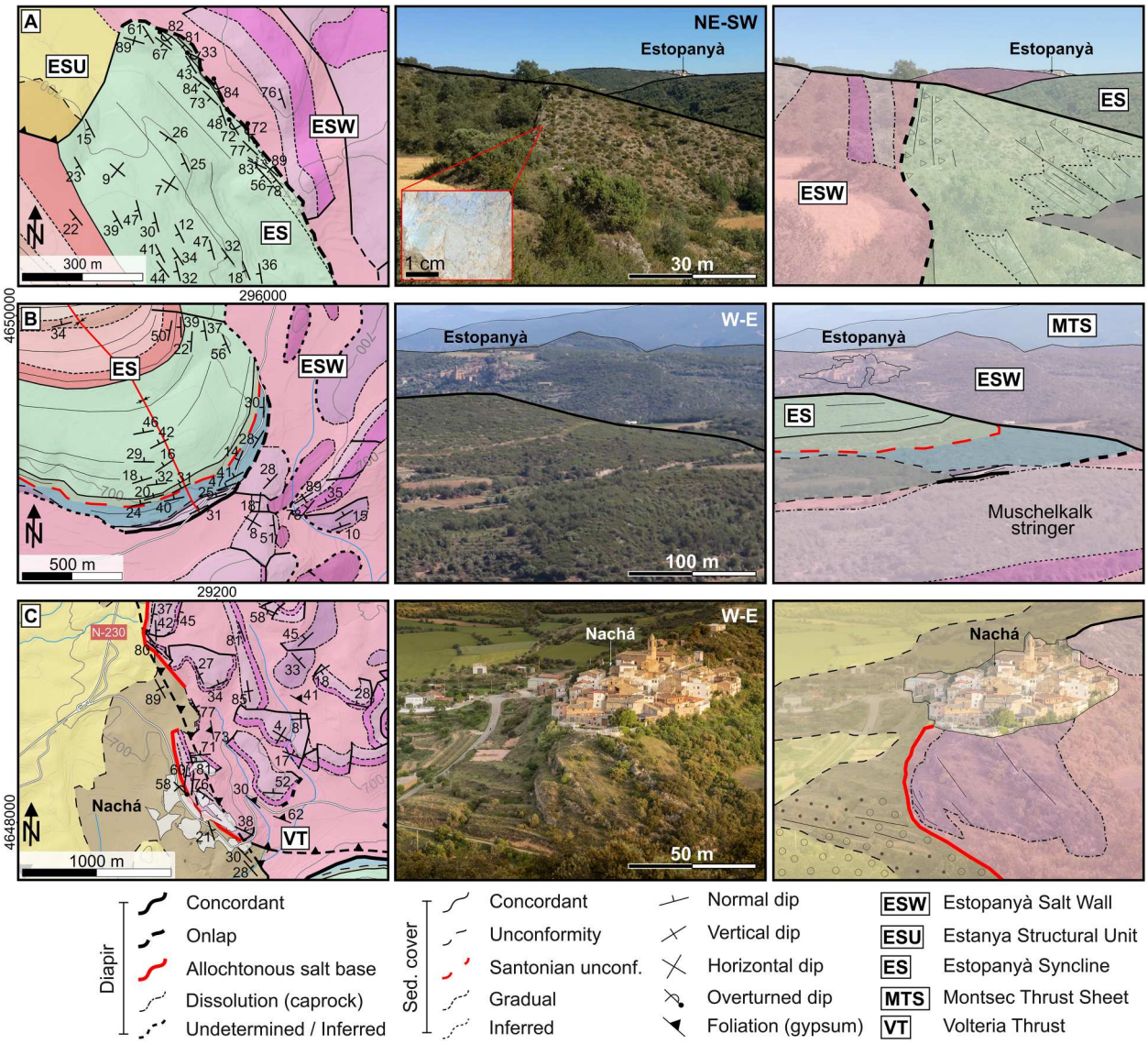

Figure 4. Field images illustrating stratigraphical contacts and geometries between diapir exposures and flanking sedimentary successions. (A) In the eastern limb of the Estopanyà Syncline, well-exposed onlap geometries are observed in the Late Cretaceous succession. The dips are sub-vertical to overturned, suggesting flap geometries affecting the Adraén and Terradets Formations. The contact between the Estopanyà Salt Wall and the Estopanyà and Boix Synclines is characterized by halokinetic breccias (red square), rapid lateral facies changes, and wedging geometries, supporting this interpretation (following Ramirez-Perez et al., 2024). (B) At the southern closure of the Estopanyà Syncline, a concordant pre-orogenic sequence is observed over diapir exposures. Northeastward, Late Triassic units are overlain by a Jurassic succession, progressively onlapping the diapir. (C) At Nachá village, an allochthonous salt body is observed in the hanging wall block of the Volteria Thrust. The imbrication of the Muschelkalk stringers in the frontal part suggest a small salt advance forming a flaring diapir with an overhanging contact over the folded Peraltilla Member (Lower Oligocene). To the north of Nachá, the salt is postdated by the Sariñena Member, constraining an Oligocene age for the salt overhang and the emplacement of the Volteria Thrust (image from Ayuntamiento de Baells – Gorka Martínez Llurda).

subdivided into NW and SW domains by a small asymmetric upright anticline (Figure 3). The eastern boundary of this anticline is a sharp contact with the Estopanyà Syncline that is often obscured by Quaternary deposits. The western termination of the anticline includes verticalized Paleocene beds placed in the footwall of the Sant Quilez back-thrust, though the contact is obscured by Oligocene conglomerates that truncate the latter Paleocene beds (Figure 3). The northern and southern closures of the anticline consist of gently dipping Paleocene strata partially covered by salt exposures (allochthonous contacts in the Main Map).

Extending to the north, the Sant Quilez back-thrust forms the western boundary of the Castilló Diapir, which is bounded by the Estopanyà Syncline in the east and by a complex area in the north predominated by a NW–SE oriented weld. The geographical centre of the diapir coincides with the Castilló del Pla village (Figure 3). Comparatively, this diapir is more polygonal than the Estopanyà Salt Wall and it contains less stringers due to its lack or because they are

covered under Quaternary deposits (see Fonz sheet, Teixell et al., 1994). In the south, the salt of the Castilló Diapir overhangs the Paleocene units of the upright anticline. The western contact of the salt is abrupt against the Sant Quilez Syncline whereas, in the east, the salt is constrained to the footwall of a normal fault that displaces the western limb of the Estopanyà Syncline in its hanging-wall (cf. Senz & Zamorano, 1992). In the north, it is difficult to trace the boundaries of the Castilló Diapir because the absence of stringers hinders to differentiate it from other salt exposures owing to the weld in the north of the study area (see Figure 3).

5. Discussion

5.1. Halokinetic stratigraphy and timing of diapirism in Estopanyà

The present-day geometry of the Estopanyà Syncline and adjacent salt structures is the result of an interplay between halokinesis and tectonic shortening during the Pyrenean orogeny.

In the eastern sector, Late Cretaceous units onlap the Estopanyà Salt Wall (Figure 4(A)). Distinctive facies such as halokinetic breccias, an absence of diapir-derived clasts in the flanking sedimentary rocks, and wedging geometries along the contact, point to salt inflation next to the Estopanyà and Boix Synclines since, at least, during the Maastrichtian (Ramirez-Perez et al., 2024). Salt inflation formed the flap geometries that characterize the Terradets and Adraén Fms on both flanks of the Estopanyà Salt Wall in this region. In the NE domain, the Ypresian units of the Estanya Structural Unit directly overlay the Estopanyà Salt Wall. This contact is also interpreted as an onlap suggesting that the Estopanyà Salt Wall was already exposed during the early to middle Ypresian, flanking laterally these carbonate platforms. The Keuper quartz grains found within the Ypresian carbonates of the Boix Syncline will additionally support diapir exposure (Ramirez-Perez et al., 2024).

The contact between the southern closure of the Estopanyà Syncline and the Estopanyà Salt Wall is interpreted as concordant attending the stratigraphical continuity between the diapiric and the non-diapiric Triassic units (Figure 4(B)). East of this point, the pre-orogenic unit wedges against the diapir, whereas to the west the contact is more complex, leading to multiple interpretations of its nature (Figure 4(B)). Probably, this contact results from a combination of an onlap of the Late Cretaceous units over both the diapir and an overhanging diapir flare. In this sense, small-scale allochthonous salt emplacements occurring along the diapir margin (i.e. salt flares) are likely suggested to occur covering the hinge of the Tragó Syncline or in the northern part of the SW closure of the Estopanyà Syncline (allochthonous contacts in the Main Map). Otherwise, the contact could also be produced by the erosion of the pre-orogenic units by the Santonian Unconformity and the onlap of the Late Cretaceous succession over the eroded flank of an inflated salt structure. Thereby, the absence of any wedging geometry, overturned strata, or halokinetic breccias, as those observed in the eastern sector of the Main Map, indicates that the most proximal part of this contact has not been preserved.

The contact between the diapir and Peraltilla Fm in Nachá provides insights into the diapir's evolution during the Oligocene. The irregular shape of the contact and the topographic position of the Triassic relative to the Peraltilla Fm (Lower Oligocene) suggest the presence of allochthonous salt at this location (Figure 4(C)). The salt is onlapped by the Sariñena Fm in the north, indicating that salt emplacement probably occurred during the Lower–Upper Oligocene, concurrently with the break-back reactivation of the SMTS frontal part (Meigs, 1997). The more extensive salt advance in Nachá compared to other mapped areas, likely reflects either (i) the occurrence of a palaeovalley (cf. Cofrade, Cantarero, et al., 2023); or (ii) that salt was transported on the hanging-wall of Volteria Thrust, elevating it over the surrounding detrital units, which is a more probable hypothesis (Teixell & Barnolas, 1996).

The contacts observed between the diapir and the flanking units in the western sector are also probably allochthonous at some points along the main normal fault trace. In this regard, due to the small area covered by the salt, it is proposed the occurrence of salt flares at the flanks of hanging diapirs. The observed onlap of the Oligocene conglomerates against the diapir in the western part of the map suggests a rapid diapir rise in Estopanyà during the Oligocene, which probably caused the observed salt flares. Similar contacts are described in other diapirs of the SMTS that were also buried during the Upper Oligocene–Miocene (Burrel & Teixell, 2021; Cofrade, Gratacós, et al., 2023; Cofrade, Závada, et al., 2023).

5.2. Evolution of diapirism in Estopanyà

The stratigraphical contacts of studied diapirs suggest that diapirism occurred at different times in the ENE and WSW sectors of the studied area.

Stratigraphical relationships in the eastern limb of the Estopanyà Syncline indicate a Late Cretaceous diapirism that evolved from shallowly buried salt-inflated structures at the time of deposition of the Terradets Fm (Maastrichtian). These structures uplift continuously during the sedimentation of the Tremp Group (Maastrichtian–Paleocene), producing a condensed succession in the Boix Syncline (Ramirez-Perez et al., 2024). The lower Eocene units onlap the

Estopanyà Salt Wall and contain diapir-derived fragments, indicating an exposure of the pre-existing diapirs as salt walls slightly before to the arrival of the compressional onset into the SMTS (Ramirez-Perez et al., 2024).

One option to explain Lower Eocene diapirism in Estopanyà is the occurrence of different scale and orientation salt-inflated structures that were reactivated or squeezed slightly before the orogenic onset. The deformation of these diapirs influenced stress distribution and subsequent diapirism in the studied area. In this sense, present-day structures in Estopanyà account for a larger shortening in the NW part of Estopanyà Syncline, involving different welds and thrusts, than in the SE, where diapirs are still preserved (Main Map). These structures in Estopanyà resemble the ones produced in models of salt deformation during tectonic shortening (e.g. Dooley et al., 2019). In them, diapirs oblique to the main contractive forces usually narrow forming secondary welds such as those of the western limb of the Estopanyà and Boix Synclines. Contrarily, diapirs oriented parallel to the shortening direction remain open extruding salt during shortening (Duffy et al., 2021; Rowan & Vendeville, 2006). Following these models, diapirs in Estopanyà should be expected to show a N–S orientation. However, the trace and position of the studied ones (e.g. the Estopanyà Salt Wall) do not completely agree this trend, being oblique to the main direction of the Pyrenean contraction (N–S).

The current position of diapirs and welds in Estopanyà could be explained by the pre-existence of comparatively wider salt walls in the ESE sector than in the WNW. During shortening, narrow salt walls were rapidly squeezed forming the present-day welds, whereas the principal diapirs do not arrive to weld due to their major extension (cf. Duffy et al., 2021). Another possibility is to consider a clockwise rotation affecting the Estopanyà Syncline during shortening, which agree with studies reporting a Middle Eocene–Oligocene rotation of the frontal structures of the South-Central Pyrenean Thrust Salient (e.g. Muñoz et al., 2013; Sussman et al., 2004). The two proposed possibilities about diapir evolution agree with accepted studies on salt basin evolution and could, therein, also have occurred in Estopanyà. Further following these works, during welding and basin rotation salt is preferentially evacuated from shortened areas (future welds) into nearby relay zones (e.g. Dooley et al., 2019; Duffy et al., 2021). Shortening and diapir squeezing since the Lower Eocene in Estopanyà was probably traduced in a similar salt flow leading to (i) the sourcing and growth of already exposed diapirs (the Estopanyà Salt Wall) and (ii) the production of new salt-inflated regions next to the welding areas, forming buried salt structures as those in the western part of the Estopanyà Syncline (the Castilló Diapir). Diapirs were reactivated during the Lower Oligocene in Estopanyà due to the break-back reactivation of the Serres Marginals Thrust Sheet and grew, at least, until the Upper Oligocene, as depicted by the contacts observed in the western part of the study area and in the northern part of the Estopanyà Salt Wall. Probably, after compression some of the previously formed secondary welds were reactivated as collapse structures, sinking the Estopanyà Syncline into the salt beneath and lowering it topographically in the hanging-wall of normal faults.

6. Concluding remarks

The structural and stratigraphical features mapped in the Estopanyà Syncline and adjacent salt bodies reveal a complex history of diapirism in this sector of the Serres Marginals Thrust Sheet of the Southern Pyrenees.

Diapirism in the eastern and western limbs of the Estopanyà Syncline occurred at different stages of the Pyrenean orogeny. In the eastern limb, the onlap of the Late Cretaceous succession on the diapiric Triassic facies and the presence of halokinetic geometries and distinctive breccias along the diapir margin indicates the inflation of a salt wall that likely extended to the southern closure of the Estopanyà Syncline. The onlap towards the diapir and the composition of the middle Ypresian limestones in the Boix Syncline suggest that the Estopanyà Salt Wall was already exposed during the Lower Eocene, slightly before the onset of the compressional shortening in the Serres Marginals Thrust Sheet.

In contrast, no stratigraphical evidence of Late Cretaceous to Ypresian diapirism is observed west of the Estopanyà Syncline. Diapirism in this sector was probably influenced by the existence of different scale and orientation diapirs around the Estopanyà Syncline since the Lower Eocene. Their welding and basin rotation (Eocene–Oligocene) likely produced salt evacuation sourcing already exposed diapirs and forming new salt-inflated structures that, during the Lower Oligocene break-back thrusting, extruded as new diapirs and allochthonous salt flares.

Software

Field data collection was conducted using FieldMove® (Petroleoum Experts Limited) software, installed on a tablet device equipped with a GPS system with a typical accuracy of ±2 m. Digital Elevation Models (DEMs) with LiDAR-based resolutions of 2 × 2 m and 5 × 5 m (provided by IGN, https://centrodedescargas.cnig.es) were integrated into the device, along with geological and topographical maps from the MAGNA 1:50,000 series (https://info.igme.es), serving as guidance layers during fieldwork.

The collected data was initially visualized in Google Earth and subsequently imported into a georeferenced digital environment using QGIS (v3.26 and 3.32), where the Main Map was constructed. Data filtering and curation were also performed in QGIS, leveraging a pre-existing cartographic database imported into the project file to fine-tune the accuracy of the Main Map. Data layers were then exported individually as vector files and merged in Inkscape (v1.2.2), where the final Main Map canvas was developed. The applied colour palette aligns with previously published geological maps from adjacent areas (e.g. Les Avellanes Diapir, Cofrade, Gratacós, et al., 2023). Structural, bedding, and lithological symbols were sourced from standard vector-based geological libraries and, when necessary, slightly adapted to enhance symbol clarity and the visibility.

Acknowledgements

PRP and GC acknowledge Dr Prokop Závada and Dr Ondřej Krýza from the Institute of Geophysics of Prague for sharing their ideas about caprock and stringer deformation during the fieldwork. PRP also acknowledge the Ayuntamiento de Baells-Nachá and Gorka Martinez Llurda for sharing images for this study. Authors acknowledge Reviewers (Dr Pedrera, Dr Pánek, and Dr Hardt) for their exhaustive review and comments that helped improving the original version of the manuscript. Authors also acknowledge Petroleum Experts (PE Limited) for sharing academic license to Universitat de Barcelona of MOVE® software and FieldMove® software for the data acquisition and visualization for the development of the structural cross-section. Authors would like to the dedicate this contribution to the memory of our friend and colleague Victoriano Pineda.

Disclosure statement

No potential conflict of interest was reported by the author(s).

Funding

Grants PID2021-12246NB funded by MICIU/AEI/10.12039/501100011033 and by FEDER, UE and the Catalan Council to the Grup Consolidat de Recerca 'Geologia Sedimentària' (2021 SGR-Cat 00349). PRP also acknowledges the support of a 'PREDOC-UB' fellowship.

Data availability statement

Data supporting the findings and discussions of this study are available within the article and its supplementary materials.

ORCID

Pedro Ramirez-Perez http://orcid.org/0000-0003-2157-4276
Gabriel Cofrade http://orcid.org/0000-0003-3329-7720
Mercè Estiarte-Ruiz http://orcid.org/0000-0003-2512-6390
Antonio Teixell http://orcid.org/0000-0002-7423-6361
Anna Travé http://orcid.org/0000-0002-2735-3733

References

Andrie, J. R., Giles, K. A., Lawton, T. F., & Rowan, M. G. (2012). Halokinetic-sequence stratigraphy, fluvial sedimentology and structural geometry of the Eocene Carroza Formation along La Popa salt weld, La Popa Basin, Mexico. *Geological Society, London, Special Publications*, *363*(1), 59–79. https://doi.org/10.1144/SP363.4

Angrand, P., Mouthereau, F., Masini, E., & Asti, R. (2020). A reconstruction of Iberia accounting for Western Tethys–North Atlantic kinematics since the late-Permian–Triassic. *Solid Earth*, *11*(4), 1313–1332. https://doi.org/10.5194/se-11-1313-2020

Beaumont, C., Muñoz, J. A., Hamilton, J., & Fullsack, P. (2000). Factors controlling the Alpine evolution of the central Pyrenees inferred from a comparison of observations and geodynamical models. *Journal of Geophysical Research: Solid Earth*, *105*(B4), 8121–8145. https://doi.org/10.1029/1999JB900390

Burbank, D. W., Vergés, J., Muñoz, J. A., & Bentham, P. (1992). Coeval hindward- and forward-imbricating thrusting in the south-central Pyrenees, Spain: Timing and rates of shortening and deposition. *Geological Society of America Bulletin*, *104*(1), 3–17. https://doi.org/10.1130/0016-7606(1992)104<0003:CHAFIT>2.3.CO;2

Burrel, L., & Teixell, A. (2021). Contractional salt tectonics and role of pre-existing diapiric structures in the Southern Pyrenean foreland fold–thrust belt (Montsec and Serres Marginals). *Journal of the Geological Society*, *178*(4), 1–14. https://doi.org/10.1144/jgs2020-085

Burrel, L., Teixell, A., Gómez-Gras, D., & Coll, X. (2021). Basement-involved thrusting, salt migration and intramontane conglomerates: A case from the Southern Pyrenees. *BSGF – Earth Sciences Bulletin*, *192*(1), 1–25. https://doi.org/10.1051/bsgf/2021013

Casas, A., Santolaria, P., Rivero, L., Casas-Sainz, A., Himi, M., Pinto, V., & Sendrós, A. (2016). The gravity method: New challenges for delineation diapiric structures in north-east Spain. *First Break*, *34*(8), 1–16. https://doi.org/10.3997/1365-2397.34.8.86173

Casini, G., Vergés, J., Drzewiecki, P., Ford, M., Cruset, D., Wright, W., & Hunt, D. (2023). Reconstructing the Iberian salt-bearing rifted margin of the Southern Pyrenees: Insights from the Organyà Basin. *Tectonics*, *42*(7), e2022TC007715. https://doi.org/10.1029/2022TC007715

Cofrade, G., Cantarero, I., Gratacós, Ò, Ferrer, O., Ramirez-Perez, P., Travé, A., & Roca, E. (2023). Allochthonous salt advance recorded by the adjacent syn-kinematic sedimentation: Example from the Les Avellanes diapir (South Central Pyrenees). *Global and Planetary Change*, *220*, 104020. https://doi.org/10.1016/J.GLOPLACHA.2022.104020

Cofrade, G., Gratacós, Ò, Cantarero, I., Ferrer, O., Ramirez-Perez, P., Roca, E., & Travé, A. (2023). Salt sheet extrusion and emplacement within the South-Central Pyrenean fold-and-thrust belt: The Les Avellanes Diapir case-of-study. *Journal of Maps*, *19*(1), 1–14. https://doi.org/10.1080/17445647.2023.2273834

Cofrade, G., Závada, P., Krýza, O., Cantarero, I., Gratacós, Ò, Ferrer, O., Adineh, S., Ramirez-Perez, P., Roca, E., & Travé, A. (2023). The kinematics of a salt sheet recorded in an array of distorted intrasalt stringers (Les Avellanes Diapir – South-Central Pyrenees). *Journal of Structural Geology*, *176*, 104963. https://doi.org/10.1016/J.JSG.2023.104963

Counts, J. W., Dalgarno, C. R., Amos, K. J., & Hasiotis, S. T. (2019). Lateral facies variability along the margin of an outcropping salt-withdrawal Minibasin, South Australia. *Journal of Sedimentary Research*, *89*(1), 28–45. https://doi.org/10.2110/JSR.2019.2

Cruset, D., Vergés, J., Muñoz-López, D., Moragas, M., Cantarero, I., & Travé, A. (2023). Fluid evolution from extension to compression in the Pyrenean Fold Belt and Basque-Cantabrian Basin: A review. *Earth-Science Reviews*, *243*, 104494. https://doi.org/10.1016/J.EARSCIREV.2023.104494

Dooley, T., Duffy, O., Hudec, M., & Fernandez, N. (2019). PS shortening of diapir provinces: Translation, tilting and rotation of minibasins in isolated minibasin systems. *change*, *2000*(2), 1–5.

Duffy, O. B., Dooley, T. P., Hudec, M. R., Fernández, N., Jackson, C. A. L., & Soto, J. I. (2021). Principles of shortening in salt basins containing isolated minibasins. *Basin Research*, *33*(3), 2089–2117. https://doi.org/10.1111/bre.12550

Duffy, O. B., Dooley, T. P., Hudec, M. R., Jackson, M. P. A., Fernández, N., Jackson, C. A. L., & Soto, J. I. (2018). Structural evolution of salt-influenced fold-and-thrust belts: A synthesis and new insights from basins containing isolated salt diapirs. *Journal of Structural Geology*, *114*, 206–221. https://doi.org/10.1016/J.JSG.2018.06.024

Duffy, O., Hudec, M., Peel, F., Apps, G., Bump, A., Moscardelli, L., Dooley, T., Fernandez, N., Bhattacharya, S., Wisian, K., & Shuster, M. (2023). The role of salt tectonics in the energy transition: An overview and future challenges. *Tektonika*, *1*(1), 18–48. https://doi.org/10.55575/tektonika2023.1.1.11

Ford, M., Masini, E., Vergés, J., Pik, R., Ternois, S., Léger, J., Dielforder, A., Frasca, G., Grool, A., Vinciguerra, C., Bernard, T., Angrand, P., Crémades, A., Manatschal, G., Chevrot, S., Jolivet, L., Mouthereau, F., Thinon, I., & Calassou, S. (2022). Evolution of a low convergence collisional orogen: A review of Pyrenean orogenesis. *BSGF – Earth Sciences Bulletin*, *193*(2), 1–41. https://doi.org/10.1051/bsgf/2022018

Gannaway Dalton, C. E., Giles, K. A., Munoz, J. A., & Rowan, M. G. (2022). Interpreting the nature of the Aulet and Adons diapirs from sedimentologic and stratigraphic analysis of flanking minibasin strata, Spanish Pyrenees, Catalunya, Spain. *Journal of Sedimentary Research*, *92*(3), 167–209. https://doi.org/10.2110/JSR.2021.179

García-Senz, J., López-Mir, B., Robador, A., Dinarès-Turell, J., & Pedrera, A. (2024). Translation, collision and vertical-axis rotation in the Organyà and Montsec minibasins (South-Central Pyrenees, Spain). *Basin Research*, *36*(1), e12846. doi:10.1111/bre.12846

García-Senz, J., Zamorano, M., Montes, M., Rico, M., & Barnolas, A. (1990). *Mapa geológico de la Hoja n° 326 (Monzón). Mapa Geológico de España 1:50000, MAGNA series*. IGME.

Garrido-Megías, A. (1972). Precisiones sobre la" mise en place" del manto de Gavarnie en el borde norte del valle del Ebro (Región de Barbastro, provincia de Huesca). *Acta Geológica Hispánica*, *7*(2), 50–52.

Garrido-Megias, A. (1973). *Estudio geologico y relacion entre tectonica y sedimentacion del secundario y terciario de la vertiente meridional pirenaica en su zona central (Provincias de Huesca y Lérida)* [PhD thesis]. Universidad de Granada.

González-Esvertit, E., Canals, À, Bons, P. D., Murta, H., Casas, J. M., & Gomez-Rivas, E. (2022). Geology of giant quartz veins and their host rocks from the Eastern Pyrenees (Southwest Europe). *Journal of Maps*, *19*(1), 1–13. https://doi.org/10.1080/17445647.2022.2133642

Jackson, M. P. A., & Hudec, M. R. (2017). *Salt tectonics: Principles and practice*. Cambridge University Press. https://doi.org/10.1017/9781139003988

Jackson, M. P. A., & Talbot, C. J. (1986). External shapes, strain rates, and dynamics of salt structures. *Geological Society of America Bulletin*, *97*(3), 305–323. https://doi.org/10.11300016-7606(1986)97<305:ESSRAD>2.0.CO;2

Jurado, M. J. (1990). El Triásico y el Liásico basal evaporíticos del subsuelo de la cuenca del Ebro. In F. Ortí & J. M. Salvany (Eds.), *Formaciones evaporíticas de la Cuenca del Ebro y cadenas penféricasyde la zona de Levante* (pp. 21–28). ENRESA-Univ.

Kalifi, A., Ribes, C., Dietrich, P., Dujoncquoy, E., Muñoz, J. A., Callot, J. P., & Ringenbach, J. C. (2023). Facies distribution along salt walls: The Upper Cretaceous mixed siliciclastic-carbonate deposits of the Cotiella minibasins (Southern Pyrenees, Spain). *Marine and Petroleum Geology*, *147*, 105989. https://doi.org/10.1016/J.MARPETGEO.2022.105989

Labaume, P., & Teixell, A. (2020). Evolution of salt structures of the Pyrenean rift (Chaînons Béarnais, France): From hyper-extension to tectonic inversion. *Tectonophysics*, *785*, 228451. https://doi.org/10.1016/J.TECTO.2020.228451

Lanaja, J. M. (1987). *Contribución de la Exploración Petrolífera al Conocimiento de la Geologia de España*. IGME.

López-Mir, B., Muñoz, J. A., & García-Senz, J. (2014). Restoration of basins driven by extension and salt tectonics: Example from the Cotiella Basin in the central Pyrenees. *Journal of Structural Geology*, *69*(PA). https://doi.org/10.1016/j.jsg.2014.09.022

López-Mir, B., Muñoz, J. A., & García-Senz, J. (2015). Extensional salt tectonics in the partially inverted Cotiella post-rift basin (south-central Pyrenees): Structure and evolution. *International Journal of Earth Sciences*, *104*(2), 419–435. https://doi.org/10.1007/s00531-014-1091-9

Martín-Martín, J. D., Vergés, J., Saura, E., Moragas, M., Messager, G., Baqués, V., Razin, P., Grélaud, C., Malaval, M., Joussiaume, R., Casciello, E., Cruz-Orosa, I., & Hunt, D. W. (2017). Diapiric growth within an Early Jurassic rift basin: The Tazoult salt wall (central High Atlas, Morocco). *Tectonics*, *36*(1), 2–32. https://doi.org/10.1002/2016TC004300

Meigs, A. J. (1997). Sequential development of selected Pyrenean thrust faults. *Journal of Structural Geology*, *19*(3–4), 481–502. https://doi.org/10.1016/S0191-8141(96)00096-X

Moragas, M., Baqués, V., Travé, A., Martín-Martín, J. D., Saura, E., Messager, G., Hunt, D., & Vergés, J. (2019). Diagenetic evolution of lower Jurassic platform carbonates flanking the Tazoult salt wall (Central High Atlas, Morocco). *Basin Research*, *32*(3), 546–566. https://doi.org/10.1111/bre.12382

Mouthereau, F., Filleaudeau, P. Y., Vacherat, A., Pik, R., Lacombe, O., Fellin, M. G., Castelltort, S., Christophoul,

F., & Masini, E. (2014). Placing limits to shortening evolution in the Pyrenees: Role of margin architecture and implications for the Iberia/Europe convergence. *Tectonics*, *33*(12), 2283–2314. https://doi.org/10.1002/2014TC003663

Muñoz, J. A. (1992). Evolution of a continental collision belt: ECORS-Pyrenees crustal balanced cross-section. In K. R. McClay (Ed.), *Thrust tectonics* (1st ed., pp. 235–236). Springer.

Muñoz, J. A., Beamud, E., Fernández, O., Arbués, P., Dinarès-Turell, J., & Poblet, J. (2013). The Ainsa Fold and thrust oblique zone of the central Pyrenees: Kinematics of a curved contractional system from paleomagnetic and structural data. *Tectonics*, *32*(5), 1142–1175. https://doi.org/10.1002/tect.20070

Muñoz, J. A., Ferrer, O., Gratacós, O., & Roca, E. (2024). The influence of the geometry of salt detachments on thrust salient development: An analogue modelling approach based on the South-Central Pyrenean thrust salient. *Journal of Structural Geology*, *180*, 105078. https://doi.org/10.1016/J.JSG.2024.105078

Muñoz, J. A., Mencos, J., Roca, E., Carrera, N., Gratacós, O., Ferrer, O., & Fernández, O. (2018). The structure of the South-Central-Pyrenean fold and thrust belt as constrained by subsurface data. *Geologica Acta*, *16*(4), 439–460. https://doi.org/10.1344/GeologicaActa2018.16.4.7

Ortí, F., Pérez-López, A., & Salvany, J. M. (2017). Triassic evaporites of Iberia: Sedimentological and palaeogeographical implications for the western Neotethys evolution during the Middle Triassic–Earliest Jurassic. *Palaeogeography, Palaeoclimatology, Palaeoecology*, *471*, 157–180. https://doi.org/10.1016/J.PALAEO.2017.01.025

Pedrera, A., García-Senz, J., Pueyo, E. L., López-Mir, B., Silva-Casal, R., & Díaz-Alvarado, J. (2023). Inhomogeneous rift inversion and the evolution of the Pyrenees. *Earth-Science Reviews*, *245*, 104555. https://doi.org/10.1016/J.EARSCIREV.2023.104555

Pichel, L. M., & Jackson, C. A.-L. (2019). *Four-dimensional variability of composite halokinetic sequences*. https://doi.org/10.31223/OSF.IO/G4K5J

Pocoví, J. A. (1978). Estudio geológico de las Sierras Marginales Catalanas (Prepirineo de Lérida). *Acta Geológica Hispánica*, *8*(3), 73–79.

Poprawski, Y., Christophe, B., Etienne, J., Matthieu, G., & Michel, L. (2016). Halokinetic sequences in carbonate systems: An example from the Middle Albian Bakio Breccias Formation (Basque Country, Spain). *Sedimentary Geology*, *334*, 34–52. https://doi.org/10.1016/j.sedgeo.2016.01.013

Puigdefàbregas, C., Muñoz, J. A., & Marzo, M. (1986). Thrust belt development in the Eastern Pyrenees and related depositional sequences in the Southern Foreland Basin. In A. Allen & P. Homewood (Eds.), *Foreland basins* (pp. 229–246). Blackwell. https://doi.org/10.1002/9781444303810.CH12

Puigdefàbregas, C., Muñoz, J. A., & Vergés, J. (1992). Thrusting and foreland basin evolution in the Southern Pyrenees. In K. R. McClay (Ed.), *Thrust tectonics* (pp. 247–254). Springer. https://doi.org/10.1007/978-94-011-3066-0_22

Ramirez-Perez, P., Cofrade, G., Cruset, D., Martín-Martín, J. D., Sizun, J. P., Onetti, E., Cantarero, I., & Travé, A. (2025). The impact of diapirism on geothermal reservoir properties of the Estopanyà and Boix synclines (South-Central Pyrenees). *Geothermal Energy*, *13*(1), 27. https://doi.org/10.1186/s40517-025-00351-8

Ramirez-Perez, P., Cofrade, G., Martín-Martín, J. D., & Travé, A. (2024). Stratigraphic evolution of a salt-walled basin: The influence of diapirism and compressional tectonics on the sedimentary record of the Estopanyà syncline (South-Central Pyrenees). *Marine and Petroleum Geology*, *163*, 106715. https://doi.org/10.1016/j.marpetgeo.2024.106715

Ribes, C., Kergaravat, C., Crumeyrolle, P., Lopez, M., Bonnel, C., Poisson, A., Kavak, K. S., Callot, J. P., & Ringenbach, J. C. (2016). Factors controlling stratal pattern and facies distribution of fluvio-lacustrine sedimentation in the Sivas mini-basins, Oligocene (Turkey). *Basin Research*, *29*(S1), 596–621. doi:10.1111/bre.12171

Roca, E., Butillé, M., Oriol, F. J., Arbués, P., De Matteis, M., Muñoz, J. A., Rowan, M., & Giles, K. (2016). *Salt tectonics and salt-sediment interaction around the Bakio Diapir, Basque-Cantabrian basin, Pyrenees*. https://doi.org/10.1190/ice2016-6384268.1

Rowan, M. G. (2017). Chapter 4 - An Overview of Allochthonous Salt Tectonics. In Permo-Triassic Salt Provinces of Europe, North Africa and the Atlantic Margins. In J. Soto, J. F. Flinch, and J. Tari (Eds.), *Tectonics and Hydrocarbon Potential* (pp. 97–114). Elsevier. https://doi.org/10.1016/B978-0-12-809417-4.00005-7

Rowan, M. G., Muñoz, J. A., Roca, E., Ferrer, O., Santolaria, P., Granado, P., & Snidero, M. (2022). Linked detachment folds, thrust faults, and salt diapirs: Observations and analog models. *Journal of Structural Geology*, *155*, 104509. https://doi.org/10.1016/J.JSG.2022.104509

Rowan, M. G., & Vendeville, B. C. (2006). Foldbelts with early salt withdrawal and diapirism: Physical model and examples from the northern Gulf of Mexico and the Flinders Ranges, Australia. *Marine and Petroleum Geology*, *23*(9–10), 871–891. https://doi.org/10.1016/J.MARPETGEO.2006.08.003

Salvany, J. M. (2017). Las formaciones yesíferas del Triásico Superior y Jurásico Inferior de Camarasa, en el frente Surpirenaico Catalán. *Estudios Geológicos*, *73*(2), 1–15. https://doi.org/10.3989/egeol.42914.460

Santolaria, P., Ayala, C., Pueyo, E. L., Rubio, F. M., Soto, R., Calvín, P., Luzón, A., Rodríguez-Pintó, A., Oliván, C., & Casas-Sainz, A. M. (2020). Structural and geophysical characterization of the Western termination of the South Pyrenean Triangle Zone. *Tectonics*, *39*(8), e2019TC005891. https://doi.org/10.1029/2019TC005891

Santolaria, P., Ayala, C., Soto, R., Clariana, P., Rubio, F. M., Martín-León, J., Pueyo, E. L., & Muñoz, J. A. (2024). Salt distribution in the South Pyrenean Central Salient: Insights from gravity anomalies. *Tectonics*, *43*(5), e2024TC008274. https://doi.org/10.1029/2024TC008274

Santolaria, P., Casas-Sainz, A. M., Soto, R., & Casas, L. (2016). Gravity modelling to assess salt tectonics in the western end of the South Pyrenean Central Unit. *Journal of the Geological Society*, *174*(2), 269–288. https://doi.org/10.1144/JGS2016-027

Santolaria, P., Casas-Sainz, A. M., Soto, R., Pinto, V., & Casas, A. (2014). The Naval diapir (southern Pyrenees): Geometry of a salt wall associated with thrusting at an oblique ramp. *Tectonophysics*, *637*, 33–44. https://doi.org/10.1016/j.tecto.2014.09.008

Santolaria, P., Ferrer, O., Rowan, M. G., Snidero, M., Carrera, N., Granado, P., Muñoz, J. A., Roca, E., Schneider, C. L., Piña, A., & Zamora, G. (2021). Influence of preexisting salt diapirs during thrust wedge evolution and secondary welding: Insights from analog

modeling. *Journal of Structural Geology*, *149*, 104374. https://doi.org/10.1016/j.jsg.2021.104374

Santolaria, P., Granado, P., Wilson, E. P., de Matteis, M., Ferrer, O., Strauss, P., Pelz, K., König, M., Oteleanu, A. E., Roca, E., & Muñoz, J. A. (2022). From salt-bearing rifted margins to fold-and-thrust belts. Insights from analog modeling and Northern Calcareous Alps case study. *Tectonics*, *41*(11), 1–27. https://doi.org/10.1029/2022TC007503

Santolaria, P., Izquierdo-Llavall, E., Soto, R., Román-Berdiel, T., & Casas-Sainz, A. (2024). Origin of oblique structures controlled by pre-tectonic thickness variations in frictional and salt-bearing fold-and-thrust belts: Insights from analogue modelling. *Journal of Structural Geology*, *179*, 105042. https://doi.org/10.1016/J.JSG.2023.105042

Santolaria, P., Vendeville, B. C., Graveleau, F., Soto, R., & Casas-Sainz, A. (2015). Double evaporitic décollements: Influence of pinch-out overlapping in experimental thrust wedges. *Journal of Structural Geology*, *76*, 35–51. https://doi.org/10.1016/j.jsg.2015.04.002

Saura, E., Ardèvol I Oró, L., Teixell, A., & Vergés, J. (2016). Rising and falling diapirs, shifting depocenters, and flap overturning in the Cretaceous Sopeira and Sant Gervàs subbasins (Ribagorça Basin, southern Pyrenees). *Tectonics*, *35*(3), 638–662. https://doi.org/10.1002/2015TC004001

Saura, E., Vergés, J., Martín-Martín, J. D., Messager, G., Moragas, M., Razin, P., Grélaud, C., Joussiaume, R., Malaval, M., Homke, S., & Hunt, D. W. (2014). Syn- to post-rift diapirism and minibasins of the Central High Atlas (Morocco): The changing face of a mountain belt. *Journal of the Geological Society*, *171*(1), 97–105. https://doi.org/10.1144/JGS2013-079

Séguret, M. (1972). *Étude tectonique des nappes et séries décollées de la partie centrale du versant sud des Pyrénées* (Vol. 2). Publications de l'Universite des Sciences et Techniques du Languedoc (USTELA).

Senz, J. G., & Zamorano, M. (1992). Evolución tectónica y sedimentaria durante el Priaboniense supe-rior-Mioceno inferior, en el frente de cabalgamiento de las Sierras Marginales occidentales. *Acta Geológica Hispánica*, *27*(1–2), 195–209.

Sussman, A. J., Butler, R. F., Dinarès-Turell, J., & Vergés, J. (2004). Vertical-axis rotation of a foreland fold and implications for orogenic curvature: An example from the Southern Pyrenees, Spain. *Earth and Planetary Science Letters*, *218*(3–4), 435–449. https://doi.org/10.1016/S0012-821X(03)00644-7

Teixell, A., & Barnolas, A. (1996). *Mapa geológico de la Hoja n° 327 (Os de Balaguer). Mapa Geológico de España 1:50000, MAGNA series*. IGME.

Teixell, A., Barnolas, A., Rosales, I., & Arboleya, M. L. (2017). Structural and facies architecture of a diapir-related carbonate minibasin (lower and middle Jurassic, High Atlas, Morocco). *Marine and Petroleum Geology*, *81*, 334–360. https://doi.org/10.1016/J.MARPETGEO.2017.01.003

Teixell, A., García-Senz, J., & Ramirez Merino, J. I. (1994). *Mapa geológico de la Hoja n° 288 (Fonz). Mapa Geológico de España 1:50000, MAGNA series*. IGME.

Teixell, A., Labaume, P., Ayarza, P., Espurt, N., de Saint Blanquat, M., & Lagabrielle, Y. (2018). Crustal structure and evolution of the Pyrenean-Cantabrian belt: A review and new interpretations from recent concepts and data. *Tectonophysics*, *724–725*, 146–170. https://doi.org/10.1016/J.TECTO.2018.01.009

Teixell, A., & Muñoz, J. A. (2000). Evolución tectono-sedimentaria del Pirineo meridional durante el Terciario: una síntesis basada en la transversal del río Noguera Ribagorçana. *Revista de La Sociedad Geológica de España*, *13*(2), 251–264.

Urai, J. L., Schléder, Z., Spiers, C. J., & Kukla, P. A. (2008). Flow and transport properties of salt rocks. In R. Littke (Ed.), *Dynamics of complex intracontinental basins: The central European basin system* (pp. 277–290). Elsevier.

Vergés, J., Moragas, M., Martín-Martín, J. D., Saura, E., Casciello, E., Razin, P., Grelaud, C., Malaval, M., Joussiame, R., Messager, G., Sharp, I., & Hunt, D. W. (2017). Salt tectonics in the Atlas Mountains of Morocco. In *Permo-Triassic salt provinces of Europe, North Africa and the Atlantic margins: Tectonics and hydrocarbon potential* (pp. 563–579. https://doi.org/10.1016/B978-0-12-809417-4.00027-6

Vergés, J., & Munoz, J. A. (1990). Thrust sequence in the southern central Pyrenees. *Bulletin de la Société géologique de France*, *VI*(2), 265–271. https://doi.org/10.2113/gssgfbull.VI.2.265

Vergés, J., Muñoz, J. A., & Martínez, A. (1992). South Pyrenean fold and thrust belt: The role of foreland evaporitic levels in thrust geometry. In K. R. McClay (Ed.), *Thrust tectonics* (pp. 255–264). Springer Netherlands.

Vidal-Royo, O., Rowan, M. G., Ferrer, O., Fischer, M. P., Fiduk, J. C., Canova, D. P., Hearon, T. E., & Giles, K. A. (2021). The transition from salt diapir to weld and thrust: Examples from the Northern Flinders Ranges in South Australia. *Basin Research*, *33*(5), 2675–2705. doi:10.1111/bre.12579

Vilar, A. (1996). *Mapa geológico de la Hoja n° 289 (Benabarre). Mapa Geológico de España 1:50000, MAGNA series*. IGME.